Bimolecular Electron Transfer in the Marcus Inverted Region

Claudia Turró, Jeffrey M. Zaleski, Yanna M. Karabatsos, and Daniel G. Nocera*

Contribution from the Department of Chemistry and the LASER Laboratory, Michigan State University, East Lansing, Michigan 48824

Received February 22, 1996⊗

Abstract: The rates for the photoinduced bimolecular reactions of a homologous series of Ru^{II} diimines with cytochrome (cyt) *c* in its oxidized and reduced forms have been measured. The electronic coupling and reorganization energy of the system have been adjusted such that the inverted region may be accessed at reasonable driving forces. The electron transfer (ET) rate constants for *Ru^{II} diimine/Fe^{II}cyt *c* reaction increase monotonically and approach the diffusion limit of 8.8×10^8 M^{-1} s^{-1} at $\Delta G° = -0.7$ V. At a higher driving force, which may be accessed with the powerfully oxidizing *Ru(diCF$_3$-bpy)$_3{}^{2+}$, the rate for ET is observed to drop off. Similarly, the high driving forces achieved with *Ru^{II} diimine/Fe^{III}cyt *c* ($-\Delta G \geq 1.12$ V) are manifested in a decrease of the ET rate constant with increasing exergonicity. The observed ET rates for both systems are well described by a bimolecular model for ET occurring over an equilibrium distribution of reactant separation distances, each having a different formation probability and weighted by the first-order ET rate constant. The unique observation of bimolecular ET in the inverted region is not due to a peculiar reaction pathway engendered by the Ru^{II} diimines, which react as do other small-molecule cations at the solvent-exposed edge of the heme. The inherent ET properties of cyt *c* engender a Marcus curve that is displaced below the diffusion limit and shifted to smaller driving forces.

Introduction

One of the most celebrated predictions of Marcus theory is that the rate of an electron transfer (ET) reaction may decrease as the free energy of the reaction increases.[1] Though long controversial, this prediction of "inverted region" ET kinetics is now well-established from experiments on systems with donor/acceptor distances fixed by protein frameworks,[2−4] covalent networks of rigid spacers,[5−14] frozen media,[15] and electrostatic complexation.[16−19] In all these cases, the distance between the donor and acceptor is constant, thus circumventing diffusion, making the ET reaction a unimolecular process. Indeed the inverted region eluded discovery prior to the early 1980s because most studies focused on bimolecular reactions.

Inverted region kinetics for bimolecular ET reactions are rare because diffusion of the reactants will conceal Marcus's classical formalism, which relates the ET rate constant, k_{et}, with the free energy of reaction, $\Delta G°$,

$$k_{et} = k_{et}(0) \exp\left[\frac{-(\lambda + \Delta G°)^2}{4\lambda k_B T}\right] \qquad (1)$$

where λ is the energy required to structurally reorganize the donor, acceptor, and their solvation spheres upon ET, and $k_{et}(0)$ is the activationless ET rate constant (for $-\Delta G° = \lambda$). Inverted region kinetics may be observed when the driving force for reaction is greater than the reorganization energy ($-\Delta G° > \lambda$). Consequently inverted region effects are most easily discerned for those reactions with small reorganization energies and large driving forces. However, even when these criteria

⊗ Abstract published in *Advance ACS Abstracts,* June 1, 1996.

(1) (a) Marcus, R. A. *J. Chem. Phys.* **1956,** *24,* 966. (b) Marcus, R. A. *Faraday Discuss. Chem. Soc.* **1960,** *29,* 21. (c) Marcus, R. A. *Annu. Rev. Phys. Chem.* **1964,** *15,* 155.

(2) (a) McLendon, G.; Miller, J. R. *J. Am. Chem. Soc.* **1985,** *107,* 7811. (b) McLendon, G. *Acc. Chem. Res.* **1988,** *21,* 160.

(3) (a) Scott, J. R.; Willie, A.; McLean, M.; Stayton, P. S.; Sligar, S. G.; Durham, B.; Millett, F. *J. Am. Chem. Soc.* **1993,** *115,* 6820. (b) Scott, J. R.; McLean, M.; Sligar, S. G.; Durham, B.; Millett, F. *J. Am. Chem. Soc.* **1994,** *116,* 7356.

(4) Dutton, P. L.; Mosser, C. C. *Proc. Natl. Acad. Sci. U.S.A.* **1994,** *91,* 10247.

(5) (a) Miller, J. R.; Calcaterra, L. T.; Closs, G. L. *J. Am. Chem. Soc.* **1984,** *106,* 3047. (b) Closs, G. L.; Calcaterra, L. T.; Green, N. J.; Penfield, K. W.; Miller, J. R. *J. Phys. Chem.* **1986,** *90,* 3673. (c) Closs, G. L.; Miller, J. R. *Science* **1988,** *240,* 440. (d) Liang, N.; Miller, J. R.; Closs, G. L. *J. Am. Chem. Soc.* **1990,** *112,* 5353.

(6) (a) Chen, P.; Duesing, R.; Tapolsky, G.; Meyer, T. J. *J. Am. Chem. Soc.* **1989,** *111,* 8305. (b) Chen, P.; Duesing, R.; Graff, D. K.; Meyer, T. J. *J. Phys. Chem.* **1991,** *95,* 5850. (c) Chen, P.; Mecklenburg, S. L.; Meyer, T. J. *J. Phys. Chem.* **1993,** *97,* 13126. (d) Katz, N. E.; Mecklenburg, S. L.; Graff, D. K.; Chen, P.; Meyer, T. J. *J. Phys. Chem.* **1994,** *98,* 8959. (e) Katz, N. E.; Mecklenburg, S. L.; Meyer, T. J. *Inorg. Chem.* **1995,** *34,* 1282.

(7) MacQueen, D. B.; Schanze, K. S. *J. Am. Chem. Soc.* **1991,** *113,* 7823.

(8) (a) Yonemoto, E. H.; Riley, R. L.; Kim, Y. I.; Atherton, S. J.; Schmehl, R. H.; Mallouk, T. E. *J. Am. Chem. Soc.* **1992,** *114,* 8081. (b) Yonemoto, E. H.; Saupe, G. B.; Schmehl, R. H.; Hubig, S. M.; Riley, R. L.; Iverson, B. L.; Mallouk, T. E. *J. Am. Chem. Soc.* **1994,** *116,* 4786.

(9) Fox, L. S.; Kozik, M.; Winkler, J. R.; Gray, H. B. *Science* **1990,** *247,* 1069.

(10) Archer, M. P.; Gadzekepo, V. P. Y.; Bolton, J. R.; Schmidt, J. A.; Weedon, A. C. *J. Chem. Soc., Faraday Trans. 2* **1986,** *82,* 2305.

(11) (a) Irvine, M. P.; Harrison, R. J.; Beddard, G. S.; Leighton, P.; Sanders, J. K. M. *Chem. Phys.* **1986,** *104,* 315. (b) Harrison, R. J.; Pearce, B.; Beddard, G. S.; Cowan, J. A.; Sanders, J. K. M. *Chem. Phys.* **1987,** *116,* 429.

(12) Wasielewski, M. R.; Niemczyk, M. P.; Svec, W. A.; Pewitt, E. B. *J. Am. Chem. Soc.* **1985,** *107,* 1080.

(13) Macpherson, A. N.; Liddell, P. A.; Lin, S.; Noss, L.; Seely, G. R.; DeGraziano, J. M.; Moore, A. L.; Moore, T. A.; Gust, D. *J. Am. Chem. Soc.* **1995,** *117,* 7202.

(14) Larson, S. L.; Cooley, L. F.; Elliott, C. M.; Kelley, D. F. *J. Am. Chem. Soc.* **1992,** *114,* 9504.

(15) (a) Beitz, J. V.; Miller, J. R. *J. Chem. Phys.* **1979,** *71,* 4579. (b) Miller, J. R.; Beitz, J. V. *J. Chem. Phys.* **1981,** *74,* 6476.

(16) (a) Gould, I. R.; Ege, D.; Moser, J. E.; Farid, S. *J. Am. Chem. Soc.* **1990,** *112,* 4290. (b) Gould, I. R.; Young, R. H.; Moody, R. E.; Farid, S. *J. Phys. Chem.* **1991,** *95,* 2068. (c) Gould, I. R.; Farid, S. *J. Phys. Chem.* **1992,** *96,* 7635. (d) Gould, I. R.; Young, R. H.; Mueller, L. J.; Albrecht, A. C.; Farid, S. *J. Am. Chem. Soc.* **1994,** *116,* 8188. (e) Arnold, B. R.; Noukakis, D.; Farid, S.; Goodman, J. L.; Gould, I. R. *J. Am. Chem. Soc.* **1995,** *117,* 4399.

(17) (a) Ohno, T.; Yoshimura, A.; Mataga, N. *J. Phys. Chem.* **1990,** *94,* 4871. (b) Segawa, H.; Takehara, C.; Honda, K.; Shimidzu, T.; Asahi, T.; Mataga, N. *J. Phys. Chem.* **1992,** *96,* 503.

(18) (a) Zhou, J. S.; Granada, E. S. V.; Leontis, N. B.; Rodgers, M. A. J. *J. Am. Chem. Soc.* **1990,** *112,* 5074. (b) Zhou, J. S.; Rodgers, M. A. J. *J. Am. Chem. Soc.* **1991,** *113,* 7728.

(19) Zou, C.; Miers, J. B.; Ballew, R. M.; Dlott, D. D.; Schuster, G. B. *J. Am. Chem. Soc.* **1991,** *113,* 7823.
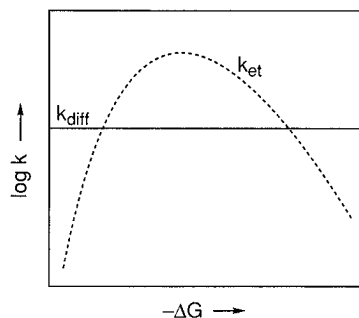
Figure 1. Parabolic dependence of the ET rate constant on the free energy driving force. The diffusion limit, signified by the horizontal solid line, truncates the parabola predicted by eq 1.

are present for a bimolecular ET reaction, the inverted region is not easily distinguished because the observed reaction rate constant has the form of a consecutive reaction mechanism consisting of diffusional (k_d) and activated (k_{act}) rate constants for electron transfer,[20-24]

$$k_{obs} = k_{act}k_d/(k_{act} + k_d) \qquad (2)$$

Activated ET can be extremely fast when $-\Delta G° = \lambda$, and the diffusion limit may impose an upper limit upon the observed reaction rate ($k_{obs} = k_d$ for $k_{act} \gg k_d$). As shown in Figure 1, the parabolic dependence predicted by eq 1 is truncated by the diffusion limit. Consequently, the observed rate constants of most bimolecular reactions display an increase with increasing free energy followed by a leveling at the diffusional limit.[25-30] Typically, the driving forces of bimolecular ET reactions have not been sufficiently energetic to permit the ET rates to lie outside the diffusion limit. Pioneering studies by Sutin and Creutz reported "vestiges" of the inverted region for the bimolecular reactions of metal polypyridyl complexes,[31] and the inverted region has been indirectly inferred from chemiluminescent bimolecular reactions.[32,33] Direct observation of inverted region behavior for a bimolecular reaction has only recently been achieved by Gray and co-workers in their studies of the back reaction between the products resulting from the quenching of an electronically excited binuclear iridium complex by pyridinium acceptors.[34]

Yet inverted region effects for bimolecular ET should not remain an isolated curiosity. With advances in the knowledge of small-molecule and protein ET reactivity during the last decade,[35-40] it should be possible to tailor important controlling factors of ET, including reorganization energies, electronic coupling, and driving force, such that the parabolic dependence predicted by eq 1 is observed for bimolecular ET. Within the context of Figure 1, this involves lowering the curve (i.e., decreasing the activationless ET rate) and shifting it to smaller driving forces (i.e., lowering the reorganization energy for ET). In addition, the role that more subtle factors play in circumventing inverted region kinetics, such as the participation of low-energy excited states in ET[41-43] and the distance dependence of the outer sphere reorganization energy,[32,44-46] may be diminished by the judicious choice of donor/acceptor systems.

The extensive work on cytochrome (cyt) *c* during the past decade[47-54] suggests that its reactions with small-molecule substrates are a suitable system to study the kinetics of bimolecular reactions in the inverted region. The reorganization energies for ET reactions of covalent and electrostatic donor/acceptor complexes of cyt *c* are modest[55,56] and primarily associated with solvent reorganization. Consistent with these findings are observations of the onset of inverted region kinetics

(20) Northrup, S. H.; Hynes, J. T. *J. Chem. Phys.* **1980**, *73*, 2700.
(21) Calef, D. F.; Wolynes, P. G. *J. Phys. Chem.* **1983**, *87*, 3387.
(22) Zusman, L. D. *Chem. Phys.* **1980**, *49*, 295.
(23) Sutin, N. *Prog. Inorg. Chem.* **1983**, *30*, 441.
(24) Morillo, M.; Cukier, R. I. *J. Chem. Phys.* **1988**, *89*, 6736.
(25) Bock, C. R.; Connor, J. A.; Buitterrez, A. R.; Meyer, T. J.; Whitten, D. G.; Sullivan, B. P.; Nagle, J. A. *J. Am. Chem. Soc.* **1979**, *101*, 4815.
(26) (a) Nocera, D. G.; Gray, H. B. *J. Am. Chem. Soc.* **1981**, *103*, 7349. (b) Marshall, J. L.; Stobart, S. R.; Gray, H. B. *J. Am. Chem. Soc.* **1984**, *106*, 3027.
(27) (a) Scandola, F.; Balzani, V.; Schuster, G. B. *J. Am. Chem. Soc.* **1981**, *103*, 2519. (b) Balzani, V.; Sabbatini, N.; Scandola, F. *Chem. Rev.* **1986**, *86*, 319.
(28) Heuer, W. B.; Totten, M. D.; Rodman, G. S.; Hebert, E. J.; Tracy, H. J.; Nagle, J. K. *J. Am. Chem. Soc.* **1984**, *106,* 1163.
(29) Kavarnos, G. J.; Turro, N. J. *Chem. Rev.* **1986**, *86*, 401.
(30) Newsham, M. D.; Cukier, R. I.; Nocera, D. G. *J. Phys. Chem.* **1991**, *95*, 9660.
(31) Creutz, C.; Sutin, N. *J. Am. Chem. Soc.* **1977**, *99*, 241.
(32) (a) Mussell, R. D.; Nocera, D. G. *J. Am. Chem. Soc.* **1988**, *110*, 2764. (b) Mussell R. D.; Nocera, D. G. *Inorg. Chem.* **1990**, *29,* 3711. (c) Mussell, R. D.; Nocera, D. G. *J. Phys. Chem.* **1991**, *95*, 6919. (d) Zaleski, J. M.; Turro, C.; Mussell, R. D.; Nocera, D. G. *Coord. Chem. Rev.* **1994**, *132*, 249.
(33) Wallace, W. L.; Bard, A. J. *J. Phys. Chem.* **1979**, *83*, 1350.
(34) (a) McCleskey, T. M.; Winkler, J. R.; Gray, H. B. *J. Am. Chem. Soc.* **1992**, *114*, 6935. (b) McCleskey, T. M.; Winkler, J. R.; Gray, H. B. *Inorg. Chim. Acta* **1994**, *225*, 319.

(35) *Electron Transfer in Biology and the Solid State*; Johnson, M. K., King, R. B., Kurtz, D. M., Jr., Kutal, C., Norton, M. L., Scott, R. A., Eds.; Advances in Chemistry Series 226; American Chemical Society: Washington, DC, 1990.
(36) *Electron Transfer in Inorganic, Organic, and Biological Systems*; Bolton, J. R., Mataga, N., McLendon, G., Eds.; Advances in Chemistry Series 228; American Chemical Society: Washington, DC, 1991.
(37) *Perspectives in Photosynthesis*; Jortner, J., Pullman, B., Eds.; Kluwer Academic Publishers: Dordrecht, 1990; Vol. 22.
(38) *Photoinduced Electron Transfer*; Fox, M. A., Chanon, M., Eds.; Elsevier: Amsterdam, 1988.
(39) *Photoinduced Electron Transfer*; Mattay, J., Ed.; Topics in Current Chemistry Series; Springer-Verlag: New York, 1991.
(40) *Metals in Biological Systems*; Sigel, H., Sigel A., Eds; Springer Verlag: New York, 1990; Vol. 27.
(41) Siders, P.; Marcus, R. A. *J. Am. Chem Soc.* **1981**, *103*, 748.
(42) Liu, D. K.; Brunschwig, B. S.; Creutz, C.; Sutin, N. *J. Am. Chem. Soc.* **1986**, *108*, 1749.
(43) Kikuchi, K.; Katagiri, T.; Niwa, T.; Takahashi, Y.; Suzuki, T.; Ikeda, H.; Miyashi, T. *Chem. Phys. Lett.* **1992**, *193*, 155.
(44) Marcus, R. A.; Siders, P. *J. Phys. Chem.* **1982**, *86*, 622.
(45) (a) Brunschwig, B. S.; Ehrenson, S.; Sutin, N. *J. Am. Chem. Soc.* **1984**, *106*, 6858. (b) Isied, S. S.; Vassilian, A.; Wishart, J. F.; Creutz, C.; Schwarz, H. A.; Sutin, N. *J. Am. Chem. Soc.* **1988**, *110*, 635. (c) Sutin, N. In *Electron Transfer in Inorganic, Organic, and Biological Systems*; Bolton, J. R., Mataga, N., McLendon, G., Eds.; Advances in Chemistry Series 228; American Chemical Society: Washington, DC, 1991; Chapter 3.
(46) Tachiya, M.; Murata, S. *J. Phys. Chem.* **1992**, *96*, 8441.
(47) (a) Winkler, J. R.; Gray, H. B. *Chem. Rev.* **1992**, *92*, 369. (b) Wuttke, D. S.; Bjerrum, M. J.; Winkler, J. R.; Gray, H. B. *Science* **1992**, *256*, 1007. (c) Meier, M.; van Eldik, R.; Chang, I.-J.; Mines, G. A.; Wuttke, D. S.; Winkler, J. R.; Gray, H. B. *J. Am. Chem. Soc.* **1994**, *116*, 1577.
(48) McLendon, G.; Hake, R. *Chem. Rev.* **1992**, *92*, 481.
(49) (a) Liang, N.; Mauk, A. G.; Pielak, G. J.; Johnson, J. A.; Smith, M.; Hoffman, B. M. *Proc. Natl. Acad. Sci. U.S.A.* **1987**, *84,* 1249. (b) Liang, N.; Mauk, A. G.; Pielak, G. J.; Johnson, J. A.; Smith, M.; Hoffman, B. M. *Science* **1988**, *240*, 311. (c) Wallin, S. A.; Stemp, E. D. A.; Everest, A. M.; Nocek, J. M.; Netzel, T. L.; Hoffman, B. M. *J. Am. Chem. Soc.* **1991**, *113*, 1842. (d) Everest, A. M.; Wallin, S. A.; Stemp, E. D. A.; Nocek, J. M.; Mauk, A. G.; Hoffman, B. M. *J. Am. Chem. Soc.* **1991**, *113*, 4337.
(50) Durham, B.; Pan, L. P.; Hahm, S.; Long, J.; Millett, F. In *Electron Transfer in Biology and the Solid State*; Johnson, M. K., King, R. B., Kurtz, D. M., Jr., Kutal, C., Norton, M. L., Scott, R. A., Eds.; Advances in Chemistry Series 226; American Chemical Society: Washington, DC, 1990; pp 181.
(51) Beratan, D. N.; Betts, J. N.; Onuchic, J. N. *Science* **1991**, *252*, 1285.
(52) (a) Moreira, I.; Sun, J.; Cho, M.-o. K.; Wishart, J. F.; Isied, S. S. *J. Am. Chem. Soc.* **1994**, *116*, 8396. (b) Sun, J.; Wishart, J. F.; Gardiner, M. B.; Cho, M.-o. P.; Isied, S. S. *Inorg. Chem.* **1995**, *34*, 3301. (c) Sun, J.; Wishart, J. F.; Isied, S. S. *Inorg. Chem.* **1995**, *34*, 3998.
(53) Conrad, D. W.; Scott, R. A. *J. Am. Chem. Soc.* **1989**, *111*, 3461.
(54) Sun, J.; Wishart, J. F.; van Eldik, R.; Shalders, R. D.; Swaddle, T. W. *J. Am. Chem. Soc.* **1995**, *117*, 2600.
(55) Meade, T. J.; Gray, H. B.; Winkler, J. R. *J. Am. Chem. Soc.* **1989**, *111*, 4353.
(56) Elias, H.; Chou, M. H.; Winkler, J. R. *J. Am. Chem. Soc.* **1988**, *110*, 429.

Table 1. Pertinent Photophysical and Energetics Data for the Reaction of Ru^{II} Diimine Complexes with Cytochrome *c* in Its Oxidized (Fe^{III}) and Reduced (Fe^{II}) States, and Observed Bimolecular ET Rate Constants

Ru^{II} diimine complex	$\tau_0/\mu s$	$E°(+/*)/V$	$E°(*/-)/V$	Fe^{II}cyt *c* + *Ru^{II}		Fe^{III}cyt *c* + *Ru^{II}	
				$-\Delta G°/V$	$k_{obs}/M^{-1}\ s^{-1}$	$-\Delta G°/V$	$k_{obs}/M^{-1}\ s^{-1}$
Ru(diOMe-phen)$_3^{2+}$	1.14	-1.20^a	0.94^a	0.69	5.68×10^8	1.45	2.08×10^8
Ru(diMe-phen)$_3^{2+}$	1.76	-1.02^b	0.65^b	0.40	2.84×10^8	1.30	2.10×10^8
Ru(phen)$_3^{2+}$	1.18	-0.87^b	0.77^b	0.52	4.36×10^8	1.12	2.65×10^8
Ru(diCF$_3$-bpy)$_3^{2+}$	0.81	-0.11^c	1.57^c	1.32	3.11×10^8	0.36	8.35×10^7

[a] Redox potentials vs NHE (±0.1 V) and excited state energies (±0.05 V) in CH$_3$CN (this work), [b] in H$_2$O (ref 58), and [c] in CH$_3$CN (ref 66).

at driving forces of ~1 eV for the fixed-distance ET reactions of cyt *c* covalently linked with Ru^{II} diimine complexes,[57] and electrostatically complexed with metalloporphyrins[18] and other redox proteins.[2] Similar reorganization energies may be expected for the bimolecular reactions of cyt *c* with small molecules. The strategy developed here is to choose a homologous series of Ru(II) diimine ET partners that possess low reorganization energies and driving forces greater than −1 V. This same strategy has been used for the observation of the inverted region for the fixed-distance, intramolecular ET reactions of Ru-modified proteins, where the replacement of hydrophilic ammine ligands of a Ru(NH$_3$)$_5$ center attached to cyt *c* at His-33 with the more hydrophobic and larger bipyridine ligands (to form a Ru(bpy)$_2$(imidazole)−His-33−cyt *c*) reduces the reorganization energy sufficiently to permit the observation of the inverted region at reasonable driving forces.[57]

We now report a systematic study of the driving-force dependence for the photoinduced bimolecular reaction of cyt *c* in its reduced and oxidized states with electronically excited Ru(II) diimine (*Ru^{II}) complexes. Systematic variation of the substituents of the parent ligand or utilization of mixed-ligand complexes allows for a wide variation of the excited state oxidation and reduction potentials,[58] which in turn control the driving force of the *Ru^{II}/cyt *c* ET reaction. Utilizing the known ET properties of cyt *c* and the Ru(II) diimine complexes, we observe inverted region behavior for the forward bimolecular ET reaction of Fe^{II} and Fe^{III} cyt *c*.

Experimental Section

Materials. Horse heart cyt *c* type VI was purchased from Sigma and was purified by standard methods.[59] The oxidized protein, dissolved in $\mu = 10$ mM, pH = 7.4 phosphate buffer, was loaded onto a CM52 (Whatman) cation exchange column and was subsequently eluted with the same buffer at a higher ionic strength ($\mu = 0.1$ M). Ferricytochrome *c* was reduced by addition of freshly prepared sodium ascorbate, or was fully oxidized with potassium ferricyanide.[60] The protein was then eluted from a Sephadex G-50 column with $\mu = 0.1$ M, pH = 5 ammonium bicarbonate buffer, to allow separation of the reducing or oxidizing agents. After the eluent was frozen with a dry ice/acetone bath, the water and buffer were removed under vacuum (10^{-3} Torr). All manipulations of Fe^{II}cyt *c* were performed under nitrogen, and the oxidation state was carefully monitored utilizing the characteristic absorption features of the protein. The reduced protein possesses a sharp absorption band at 550 nm ($\epsilon = 27.7$ mM^{-1} cm^{-1}),[61] whereas a broad feature at 530 nm ($\epsilon = 10.1$ mM^{-1} cm^{-1}) is observed for the protein in its oxidized state.[62]

The ligands, 1,10-phenanthroline (phen), 4,7-dimethyl-1,10-phenanthroline (diMe-phen), 4,7-dihydroxy-1,10-phenanthroline (diOH-phen), and 4,7-di(*p*-phenylsulfonate)-1,10-phenanthroline (BPS), were purchased from Aldrich. The ligand 4,7-dimethoxy-1,10-phenanthroline (diOMe-phen) was synthesized by treating 4,7-dichloro-1,10-phenanthroline (prepared from diOH-phen)[63] with NaOMe in benzene.[64] The ligand was characterized by ^{1}H NMR (δ, ppm, *A*, int area) (aromatic, 8.90, 5.66; 8.22, 6.11; 7.25, 5.80; OCH$_3$, 4.15, 19.6) and melting point (200 °C).

The Ru(II) diimine complexes were prepared by reported techniques.[58,65] Typically RuCl$_3$ was refluxed in ethanol/water (80/20) with 6 equiv of ligand, L, to form the red-orange RuL$_3^{2+}$ complexes. After evaporation of the solvent, the product was readily precipitated from acetone with ether. The Ru(II) complexes were characterized by comparison with their known electronic absorption and emission spectra, emissive lifetimes, and redox potentials.[58] The 4,4′-bis(trifluoromethyl)-2,2′-bipyridine complex, Ru(diCF$_3$-bpy)$_3^{2+}$, was prepared and characterized by Professor M. Furue[66] and was generously provided to us from his labs.

Methods and Instrumentation. Rate constants for the quenching of the Ru^{II} diimine excited states by cyt *c* were obtained by lifetime and transient absorption measurements using laser instrumentation that has previously been described.[67,68] Stock solutions (25 or 50 mL) containing 6×10^{-5} M of Ru^{II} complex were prepared in $\mu = 0.1$ M, pH = 7.4 phosphate buffer. The protein was dissolved in 200 μL of stock solution and placed in a 1 mm path length cuvette equipped with a stopcock. The protein concentration was varied by addition of known volumes of stock solution to the initial 200 μL protein solution. Solutions were deoxygenated by bubbling with nitrogen. The concentration of cyt *c* was determined prior to each lifetime measurement from the absorbance at either 530 or 550 nm, depending on the protein's oxidation state, and was corrected for the absorbance of the Ru^{II} complex at each wavelength (typically 0.05−0.07). In this manner, the concentration of the Ru^{II} complex remained constant over the course of an experiment.

Results and Discussion

Table 1 lists the lifetime and excited state redox potentials of a homologous series of Ru^{II} diimine complexes. The electron-withdrawing or -donating abilities of the substituents on the aromatic imine skeleton permit a wide range of driving forces to be achieved for the bimolecular reaction of the Ru^{II} diimines with cyt *c*. The long-lived excited states of all the Ru^{II} complexes are quenched by Fe^{II} and Fe^{III}cyt *c* with the rate constants shown in Table 1, as determined by the Stern−Volmer lifetime quenching method. Exemplary Stern−Volmer plots for the quenching of the MLCT excited state of Ru(diMe-phen)$_3^{2+}$ by both redox states of the protein are shown in Figure

(57) Chang, I.-J.; Gray, H. B.; Winkler, J. R. *J. Am. Chem. Soc.* **1991**, *113*, 7056.

(58) Juris, A.; Balzani, V.; Barigelletti, F.; Campagna, S.; Belser, P.; Von Zelewsky, A. *Coord. Chem. Rev.* **1988**, *84*, 85.

(59) Brautigan, D. L.; Ferguson-Miller, S.; Margoliash, E. *Methods Enzymol.* **1978**, *53*, 128.

(60) Stellwagen, E.; Cass, R. D. *J. Biol. Chem.* **1975**, *250*, 2095.

(61) Vanderkooi, J. M.; Adar, F.; Erecinska, M. *Eur. J. Biochem.* **1976**, *64*, 381.

(62) Wikström, M.; Krab, K.; Saraste, M. In *Cytochrome Oxidase: A Synthesis;* Academic Press: New York, 1981.

(63) Snyder, H. R.; Freier, H. E. *J. Am. Chem. Soc.* **1946**, *68*, 1320.

(64) Rund, J. V.; Claus, K. G. *J. Am. Chem. Soc.* **1967**, *89*, 2256.
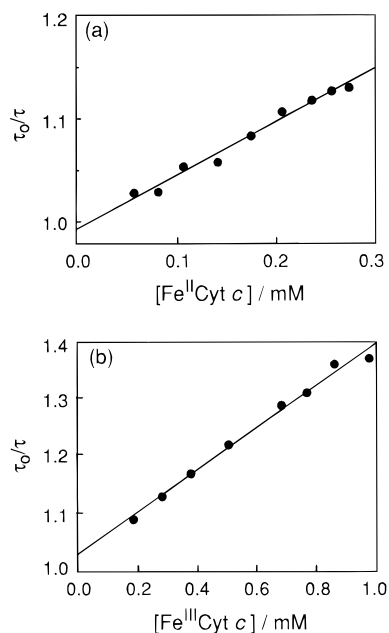
(65) Krause, R. A. *Inorg. Chim. Acta* **1977**, *22*, 209.

(66) Furue, M.; Maruyama, K.; Oguni, T.; Naiki, M.; Kamachi, M. *Inorg. Chem.* **1992**, *31*, 3792.

(67) Shin, Y.-g. K.; Miskowski, V. M.; Nocera, D. G. *Inorg. Chem.* **1990**, *29*, 2308.

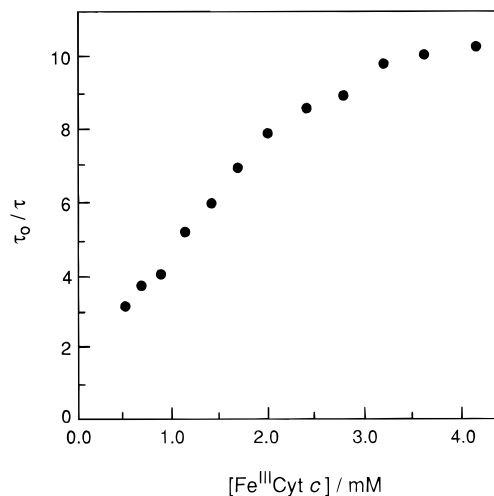(68) Jackson, J. A.; Turró, C.; Newsham, M. D.; Nocera, D. G. *J. Phys. Chem.* **1990**, *94*, 4500.

(69) Balzani, V.; Moggi, L.; Manfrin, M. F.; Bolletta, F. *Coord. Chem. Rev.* **1975**, *15*, 321.

Figure 2. Stern−Volmer plot of the quenching of electronically excited Ru(diMe-phen)$_3^{2+}$ (6.0 × 10^{-5} M) by (a) Fe^{II}cyt c and (b) Fe^{III}cyt c in $\mu = 0.1$ M phosphate buffer (pH = 7.0).

2. As predicted for a bimolecular reaction,[69] the Stern−Volmer plots for all of the quenchers are linear and exhibit an intercept of unity. The bimolecular kinetics for this system are ensured by the properties of the Ru^{II} diimine series. In contrast to anionic reactants,[2a,48,70,71] the cationic Ru^{II} complexes do not associate at the large patches of positive charge near the heme's solvent-exposed edge. Consequently, a mechanism involving binding of the small-molecule reactant with the protein followed by a quenching reaction is disfavored for the Ru^{II} diimine series. Accordingly, Stern−Volmer saturation kinetics in which the quenching rate constant becomes independent of quencher concentration, as is observed for negatively charged reactants,[18,72] are absent in our system. Indeed, such nonlinear behavior is uncovered for the Ru^{II} diimines when anionic ligands impart an overall negative charge on the complex. Figure 3 shows the Stern−Volmer plot for the quenching reaction of Ru(BPS)$_3^{4-}$ and Fe^{III}cyt c. The saturation kinetics induced by association of the anionic Ru^{II} complex to the protein is clearly apparent with a leveling of the quenching rate constant at Fe^{III}-cyt c:Ru(BPS)$_3^{4-}$ concentrations greater than 1:1.

The transient absorption spectra for the quenching reaction between the *Ru^{II} diimines and cyt c are consistent with ET products.[73,74] The transient difference spectrum accompanying the Stern−Volmer experiment summarized by Figure 4 shows the characteristic absorbance of Fe^{II}cyt c at 550 nm. The appearance of the Fe^{II}cyt c transient shown in Figure 4 occurs over the same time scale for the Stern−Volmer quenching of the Ru^{II} diimine excited state. These results are consistent with

(70) (a) Drake, P. L.; Hartshorn, R. T.; McGinnis, J.; Sykes, A. G. *Inorg. Chem.* **1989**, *28*, 1361. (b) Armstrong, G. D.; Chamber, J. A.; Sykes, A. G. *J. Chem. Soc., Dalton Trans.* **1986**, 755.
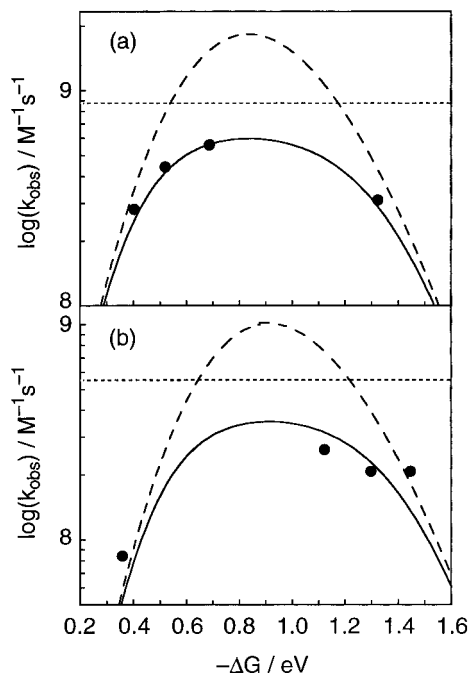
(71) (a) Butler, J.; Chapman, S. K.; Davies, D. M.; Sykes, A. G.; Speck, S. H.; Osheroff, N.; Margoliash, E. *J. Biol. Chem.* **1983**, *258*, 6400. (b) Augustin, M. A.; Chapman, S. K.; Davies, D. M.; Sykes, A. G.; Speck, S. H., Margoliash, E. *J. Biol. Chem.* **1983**, *258*, 6405.

(72) Brunschwig, B. S.; DeLaive, P. J.; English, A. M.; Goldberg, M.; Gray, H. B.; Mayo, S. L.; Sutin, N. *Inorg. Chem.* **1985**, *24*, 3743.

(73) (a) Nocera, D. G.; Winkler, J. R.; Yocom, K. M.; Bordignon, E.; Gray, H. B. *J. Am. Chem. Soc.* **1984**, *106*, 5145. (b) Winkler, J. R.; Nocera, D. G.; Yocom, K. M.; Bordignon, E.; Gray, H. B. *J. Am. Chem. Soc.* **1982**, *104*, 5798.

(74) Cho, K. C.; Che, C. M.; Cheng, F. C.; Choy, C. L. *J. Am. Chem. Soc.* **1984**, *106*, 6843.

Figure 3. Stern−Volmer plot of the quenching of electronically excited Ru(BPS)$_3^{4-}$ (6.0 × 10^{-5} M) by Fe^{III}cyt c in $\mu = 0.1$ M phosphate buffer (pH = 7.0).
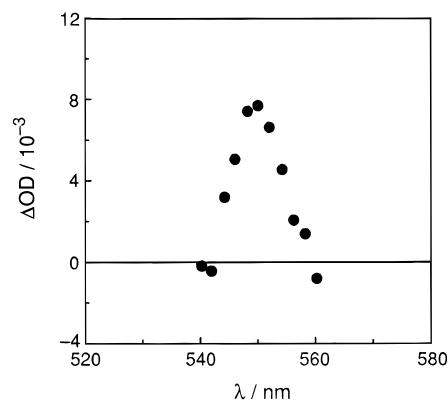
Figure 4. Transient difference spectrum of an aqueous solution buffered by phosphate ($\mu = 0.1$ M, pH = 7.0) containing Fe^{III}cyt c (8.1 × 10^{-4} M) and Ru(diMe-phen)$_3^{2+}$ (1.4 × 10^{-4} M). The difference spectrum was recorded 7 μs after a 450 nm excitation pulse.

quenching by simple one-electron transfer. At the concentration of Fe^{III}cyt c (8.1 × 10^{-4} M) utilized in the transient absorption experiment shown in Figure 4, the emission lifetime decreases by 23%. If ET is the sole source of excited state quenching in these systems, then the concentration of redox products is expected to be 1.6 × 10^{-6} M. From the measured ΔOD = 0.008 (for a 0.2 cm path length) in Figure 4, and molar extinction coefficients for Fe^{II}cyt c and Fe^{III}cyt c at 550 nm of 27 700 M^{-1} cm^{-1} and 3300 M^{-1} cm^{-1}, respectively, we obtain a Fe^{II}-cyt c concentration of 1.6 × 10^{-6} M with an error of ±20%. Thus, comparison of the lifetime quenching of *Ru(diMe-phen)$_3^{2+}$ by Fe^{III}cyt c to the formation of the reduced product, Fe^{II}cyt c, as determined by transient spectroscopy reveals that quenching proceeds exclusively by ET.

Figure 5 plots the observed ET rates vs driving force for all the reactions. The trend in the rate constants may be understood in terms of eq 2, where the overall observed rate for bimolecular reaction comprises contributions of both diffusion and activated ET. The diffusion rate component is given by[75]

$$k_{\text{diff}} = \frac{4\pi ND}{1000}\left[\int_r^\infty \mathrm{d}r\, \mathrm{e}^{[-U(r)/k_\mathrm{B}T]}r^{-2}\right]^{-1} \quad (3)$$

where the intermolecular potential between reactants, $U(r)$, is evaluated to a center-to-center separation between reactants, r,

(75) Smoluchowski, M. V. *Z. Phys. Chem.* **1917**, *92*, 129.

Figure 5. Semilog plots of k_{obs} vs the free energy driving force for the bimolecular ET between *Ru^{II} diimine complexes (Table 1) and (a) Fe^{II}cyt c and (b) Fe^{III}cyt c. The calculated fits of eqs 3–10 (integrated over $r = \infty$ to 23 Å, $\beta = 1.2$ Å, $V(0) = 200$ cm^{-1}) are illustrated for k_{obs} (solid curve), k_{diff} (dotted line), and k_{act} (dashed curve).

N is Avogadro's number, and D is the sum of the diffusion coefficients of the reactants given by the Stokes–Einstein relationship.[76] When both ET partners are charged, as is the case here, the intermolecular potential is dominated by the electrostatic forces between reactants. For two spheres, which is a good geometric description of the cyt c and Ru^{II} diimine reactants, $U(r)$ can be described within a Debye–Hückel formalism as[81]

$$U(r) = \frac{z_1 z_2 e^2}{D_s r (1 + \beta_{DH} r \sqrt{\mu})} \quad (4)$$

where z_1 and z_2 are the charges on each reactant, e is the charge on the electron, D_s is the static dielectric constant of the solvent, and μ is the ionic strength; β_{DH} is given by

$$\beta_{DH} = \left[\frac{8\pi N e^2}{1000 D_s k_B T}\right]^{1/2} \quad (5)$$

In regard to the activated rate in eq 2, the bimolecular ET reaction depends implicitly on the reactants, assuming an internuclear configuration appropriate for the ET event to take place. Sutin has treated this case with a precursor model in

(76) The diffusion coefficient for reactant A is given by $D_A = k_B T/6\pi r_A \eta$ where k_B is Boltzmann's constant, T is the temperature, r_A is the reactant's radius, and η is the viscosity of the water (= 0.89 g cm^{-1} s^{-1}). From this expression we calculate diffusion coefficients of 1.49×10^{-6} and 3.76×10^{-6} cm^2 s^{-1} for cyt c and the Ru^{II} diimines, respectively. The latter value was calculated assuming an average radius of 6.5 Å for the complex. These values compare well to the reported diffusion coeffcients of 1.1×10^{-6} and 2.0×10^{-6} cm^2 s^{-1} for cyt c[77,78] and 6.0×10^{-6} and 3.72×10^{-6} cm^2 s^{-1} for Ru^{II} and Fe^{III} diimines, respectively.[79,80]

(77) Albery, W. J.; Eddowes, M. J.; Hill, H. A. O.; Hillman, A. R. *J. Am. Chem. Soc.* **1981**, *103*, 3904.

(78) Santucci, R.; Reinhard, H.; Brunou, M. *J. Am. Chem. Soc.* **1988**, *110*, 8536.

(79) Buttry, D. A.; Anson, F. C. *J. Electroanal. Chem.* **1981**, *130*, 333.

(80) Zimonyi, M.; Ruff, I. *Electrochim. Acta* **1973**, *18*, 515.

(81) Debye, P. *Trans. Electrochem. Soc.* **1942**, *82*, 265.

which the ET rate is mediated by the equilibrium constant for the formation of a reactive complex at distance r (i.e., $k_{act} = K_p(r)k_{et}(r)$).[82] For most bimolecular reactions it is assumed that ET at distances larger than contact is negligible, and therefore the evaluation of k_{act} reduces to a fixed-distance problem at $r = \sigma$ (σ is the sum of the reactants' radii, the contact distance). However, we were concerned that the work associated with bringing the positively charged reactants together for the systems reported here would be significant, and consequently ET at distances larger than $r = \sigma$ might contribute to the overall observed rate. The activation-controlled rate constant for a bimolecular reaction occurring over a range of distances is obtained by integrating over the equilibrium distribution of reactant separation distances, each having a different formation probability given by $g_e(r)$ (from $r = \infty$ to r) and weighted by the first-order ET rate constant $k_{et}(r)$,[23,44,83]

$$k_{act} = \frac{4\pi N}{1000}\int_r^{\infty} dr\, g_e(r)\, k_{et}(r)\, r^2 \quad (6)$$

For ionic reactants in dilute solution, the equilibrium distribution function, $g_e(r)$, is described by an electrostatic potential

$$g_e(r) = \exp[-U(r)/k_B T] \quad (7)$$

with $U(r)$ defined by eq 4. For $k_{et}(r)$, we have chosen to use the semiclassical expression popularized by Closs and Miller,[5,15]

$$k_{et}(r) = \\ \frac{2\pi}{h}\left[\frac{1}{\lambda_s k_B T}\right]^{1/2}|V|^2\sum_{w=0}^{\infty}\frac{e^{-S}S^w}{w!}\exp\left\{\frac{-(\lambda_s + \Delta G + wh\nu)^2}{4\lambda_s k_B T}\right\} \quad (8)$$

where the total reorganization energy is composed of solvational λ_s and vibrational λ_v contributions with $S = \lambda_v/h\nu$, ν is the high-energy vibrational frequency associated with the acceptor, V is the electronic coupling, and w is the density of product vibrational levels.[84] This expression for $k_{et}(r)$ is central to our studies because it accounts for nuclear tunneling in the inverted region to excited vibrational states of the acceptor, which is significant for highly exergonic ET reactions.[85] The total driving force, ΔG, includes electrostatic corrections to $\Delta G°$ (Table 1) for the work required to bring products and reactants together ($\Delta G = \Delta G° - w_p - w_r$) as described by eq 4.

The solvation reorganization energy, λ_s, has contributions from the solvent (λ_{sol}) and the protein (λ_p) milieu. The former can be estimated from the classical dielectric continuum model[1,86]

$$\lambda_{sol} = (\Delta e)^2\left[\frac{1}{2r_A} + \frac{1}{2r_B} - \frac{1}{r}\right]\left[\frac{1}{D_{op}} - \frac{1}{D_s}\right] \quad (9)$$

where D_{op} and D_s are the optical and static dielectric constants of the solvent ($D_{op}(H_2O) = 1.77$, $D_s(H_2O) = 78.5$), respectively, and r_A and r_B are the reactants' radii. Because the protein radius is large compared to the Ru^{II} diimine complexes, λ_{sol} shows a much smaller distance dependence than that observed for small-molecule reactants.[29,45] The contribution from the peptide

(82) (a) Brown, G. M.; Sutin, N. *J. Am. Chem. Soc.* **1979**, *101*, 883. (b) Sutin, N. *Acc. Chem. Res.* **1982**, *15*, 275.

(83) Newton, M. D.; Sutin, N. *Annu. Rev. Phys. Chem.* **1984**, *35*, 437.

(84) Kuki, A. In *Long-Range Electron Transfer in Biology*; Structure and Bonding; Clarke, M. J., Goodenough, J. B., Jørgenson, C. K., Neilands, J. B., Reinen, D., Weiss, R., Eds.; Springer-Verlag: Berlin, 1991; Vol. 75, p 58.

(85) Liang, N.; Miller, J. R.; Closs, G. L. *J. Am. Chem. Soc.* **1990**, *112*, 5353.

(86) Marcus, R. A.; Sutin, N. *Biochim. Biophys. Acta* **1985**, *811*, 265.

matrix for Fe^{II} and Fe^{III}cyt c has been calculated to be 0.2 eV,[87] which may be directly added to the solvent reorganization at a given r to give the total outer sphere reorganization energy, λ_s.[88]

The distance dependence of V is exponential and given by[86]

$$V = V(0) \exp[-\beta/2(d-d_0)] \qquad (10)$$

where d is the edge-to-edge distance between the Ru^{II} diimine and the heme of the protein and acceptor and $V(0)$ is the value of V at $d = d_0$, which has been defined to be 3 Å to account for the electron clouds about the outermost atoms of each reactant.[47a,86] For cyt c, β is 1.2 $Å^{-1}$ and $V(0)$ is 200 cm^{-1}.[47a,51,89] It is well established that the ET reactions of cationic metal complexes featuring hydrophobic ligation spheres proceed at the exposed heme edge of the protein.[90,91] Singly modified peptide and NMR studies show that positively charged reactants access the recessed heme edge near Lys-27,[70,71,92] thereby permitting us to relate the edge-to-edge ET distance, d, in eq 10, to the protein and Ru^{II} diimine center-to-center distance, r. The distance from the outermost meso position of the heme to the center of the protein, determined from the crystal structure of cyt c, corresponds to 9.1 Å.[93] This distance leads directly to the relation $r = d - 9.1$ Å $- r_B$, where r_B is the Ru^{II} diimine radius of 6.5 Å.

With eqs 3−10 parametrically defined in r, the ET distance for the reaction of the Ru^{II} diimines with cyt c may be directly calculated by solving eqs 3 and 6. The semilog plots of the calculated rate constants, determined by evaluating eqs 3−10 for $r = \infty$ to $r = 23$ Å, vs $\Delta G°$ are shown by the solid lines in Figure 5 along with the experimentally determined rate constants of the $*Ru^{II}/Fe^{II}$cyt c and $*Ru^{II}/Fe^{III}$cyt c systems. The activated (eq 6, dashed line) and diffusion (eq 3, dotted line) rate constants composing k_{obs}, as described by eq 2, are also shown for convenience. The ET distance of 23 Å corresponds to a ligand edge-to-heme edge ET distance of 7.4 Å. This edge-to-edge distance has been observed for the bimolecular reactions of other small-molecule ET partners with cyt c;[94] accordingly, calculations using distances of closest approach other than 7.4 Å yield curves that are not consistent with the observed data. In our calculations, eq 6 was evaluated by choosing the quantum-mechanical vibrational frequency to be the 1372 cm^{-1} breathing vibration of the heme[95,96] and a vibrational reorganization energy for cyt c of 0.2 eV.[55] It is important to emphasize that the parameters employed in our calculation of the ET rate constants for both systems, $*Ru^{II}/Fe^{II}$cyt c and $*Ru^{II}/Fe^{III}$cyt c, were identical, with the exception of the charges on the reactants and products, which manifests itself in different values of k_{diff} for the two systems (indicated by the different diffusion limits in

panels a and b of Figure 5). Inspection of Figure 5a,b reveals that k_{diff} contributes significantly to the observed rate, and therefore k_{obs} parallels the rate of diffusion near its maximum; the contribution of k_{act} leading to a sharp parabolic dependence of k_{obs} is diminished significantly by the diffusion limit. From eq 8, the calculated curve exhibits a maximum when $\lambda_s = \Delta G + w_r - w_p + wh\nu$. Accounting for the work terms and $wh\nu$, we find from Figure 5a,b that the reorganization energies for the $*Ru^{II}/Fe^{II}$cyt c and $*Ru^{II}/Fe^{III}$cyt c reactions are 0.87 and 0.88 eV, respectively. These values accord well with the reorganization energies of other ET reactions involving cyt c.[18,45a,55,97,98]

The calculated ET curves and the observed ET rate constants for the reaction of $*Ru^{II}$ with Fe^{II} and Fe^{III}cyt c are in good agreement. For the former reaction, the rate constants for the $Ru(diOMe\text{-}phen)_3^{2+}$, $Ru(diMe\text{-}phen)_3^{2+}$, and $Ru(phen)_3^{2+}$ systems lie in the normal region (Figure 5a). Conversely, the high oxidation potential of $*Ru(diCF_3\text{-}bpy)_3^{2+}$ places its ET reaction in the inverted region. As predicted, the experimentally measured rate constant for this system is reduced and it is accurately predicted by the formalism established by eqs 2−10 in the inverted regime. The overall trend is reversed for the ET reactivity of $*Ru^{II}$ complexes and Fe^{III}cyt c. The reaction of Fe^{III}cyt c with $*Ru(diCF_3\text{-}bpy)_3^{2+}$ is in the normal region whereas the corresponding reactions of $*Ru(diOMe\text{-}phen)_3^{2+}$, $*Ru(diMe\text{-}phen)_3^{2+}$, and $*Ru(phen)_3^{2+}$ lie in the inverted region. As shown in Figure 5b, with the exclusion of the $Ru(diOMe\text{-}phen)_3^{2+}$ system, the data and the calculated curve are consonant. An ET rate that is faster than predicted for the $Ru(diOMe\text{-}phen)_3^{2+}$/cyt c system suggests that this highly energetic ET reaction is mediated by the formation of the Fe^{II}cyt c (^{3}MLCT) excited state ($\Delta E = 1.05$ eV).[99] This behavior has been observed for $*Ru^{II}-Fe^{III}$cyt $c \to *Ru^{III}-Fe^{II}$cyt c and $Ru^{I}-Fe^{III}$cyt $c \to Ru^{II}-Fe^{II}$cyt c when the driving forces of these intramolecular reactions exceed -1.25 V. As shown by Figure 5b, the rate/energy leveling occurs at a similar potential for the bimolecular reaction of Fe^{III}cyt c with $*Ru^{II}$.

Several important features in Figure 5 pertain to the ET reactivity of cyt c with $*Ru^{II}$ complexes. The observed rate constants for the bimolecular reaction of $*Ru^{II}$ with Fe^{II} and Fe^{III}cyt c, in the inverted and normal regions, are completely described by a formalism that accounts for ET occurring over an equilibrium distribution of distances. The treatment is detailed enough to not only reveal the inverted region but also unveil subtle mechanistic features within it such as the importance of protein excited states in mediating highly energetic ET. The deviation of the observed rate constants from predicted inverted behavior occurs at the same energy in both unimolecular and bimolecular reactions of Fe^{III}cyt c. That this mechanism does not depend on the molecularity of the reaction is understandable since it involves the same ^{3}MLCT excited state of protein for both uni- and bimolecular reactions and it is a satisfying consequence of our analysis. Another important feature of Figure 5 is that the appropriate behavior is observed for the $Ru(diCF_3\text{-}bpy)_3^{2+}$ system, which contrasts that of most $*Ru^{II}$ reagents. For the $*Ru^{II}/Fe^{II}$cyt c reaction, $Ru(diCF_3\text{-}bpy)_3^{2+}$ is inverted whereas the other $*Ru^{II}$ complexes with their more typical excited state potentials lie in the normal region. For the $*Ru^{II}/Fe^{III}$cyt c system, the opposite behavior is observed. Because inverted and normal region kinetics are

(87) Churg, A. K.; Weiss, R. M.; Warshel, A.; Takano, T. *J. Phys. Chem.* **1983**, *87*, 1683.

(88) Betrand, P. In *Long-Range Electron Transfer in Biology*; Structure and Bonding; Clarke, M. J., Goodenough, J. B., Jørgenson, C. K., Neilands, J. B., Reinen, D., Weiss, R., Eds.; Springer-Verlag: Berlin, 1991; Vol. 75, p 26.

(89) Gray, H. B.; Winkler, J. R. *Pure Appl. Chem.* **1992**, *64*, 1257.

(90) Wherland, S.; Gray, H. B. In *Biological Aspects of Inorganic Chemistry*; Addison, A. W., Cullen, W. R., Dolphin, D., James, B. R., Eds.; Wiley-Interscience: New York, 1977; p 289.

(91) Louie, G. V.; Brayer, G. D. *J. Mol. Biol.* **1990**, *214*, 527.

(92) (a) Butler, J.; Davies, D. M.; Sykes, A. G.; Koppenol, W. H.; Osheroff, N.; Margoliash, E. *J. Am. Chem. Soc.* **1981**, *103*, 469. (b) Butler, J.; Koppenol, W. H.; Margoliash, E. *J. Biol. Chem.* **1982**, *257*, 10747.

(93) Brookhaven Protein Data Bank; Brookhaven National Laboratories, Upton, NY.

(94) Mauk, A. G.; Scott, R. A.; Gray, H. B. *J. Am. Chem. Soc.* **1980**, *102*, 4360.

(95) Stallard, B. R.; Callis, P. R.; Champion, P. M.; Albrecht, A. C. *J. Chem. Phys.* **1984**, *80*, 70.

(96) Simpson, M. C.; Millett, F.; Fan, B.; Ondrias, M. R. *J. Am. Chem. Soc.* **1995**, *117*, 3296.

(97) Dixon, D. W.; Hong, X.; Woehler, S. E.; Mauk, A. G.; Sishta, B. P. *J. Am. Chem. Soc.* **1990**, *112*, 1082.

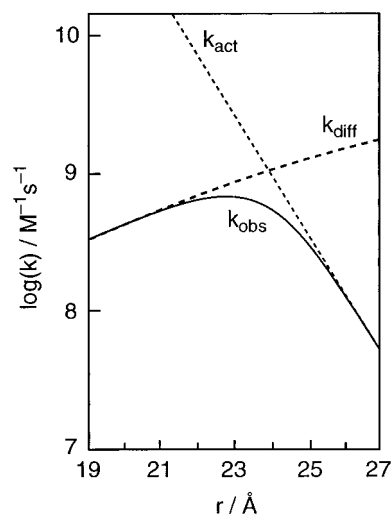(98) McLendon, G.; Pardue, K.; Bak, P. *J. Am. Chem. Soc.* **1987**, *109*, 7540.

(99) Mines, G. A.; Bjerrum, M. J.; Hill, M. G.; Casimiro, D. R.; Chang, I.-J.; Winkler, J. R.; Gray, H. B. *J. Am. Chem. Soc.* **1996**, *118*, 1961.
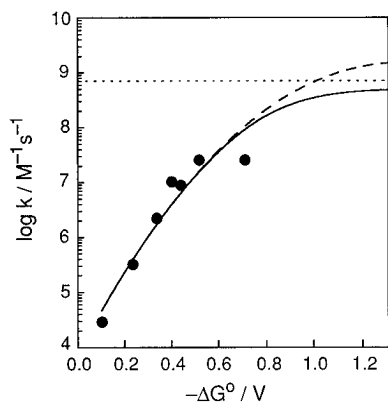
Figure 6. The observed ET rate constants plotted vs $-\Delta G$ for the reaction of $^3Zn^{II}$ cyt c with a series of viologen quenchers; these data were taken from ref 102. The rate constants k_{obs} (solid curve), k_{act} (dashed curve), and k_{diff} (dotted line) are calculated by evaluating eqs 3–10 with the same parameters used to generate the respective curves displayed in Figure 5, with the only modification being the average radius of the quencher (6.5 Å for the Ru^{II} diimine complexes and 3.5 Å for the viologen quenchers).

observed for $^*Ru^{II}/Fe^{II}$cyt c and for $^*Ru^{II}/Fe^{III}$cyt c, bimolecular ET in the inverted region is not a peculiarity of the nature of the redox process or the $^*Ru^{II}$ complexes.

Our analysis may be generalized to bimolecular ET reactions of cyt c with other small molecules including inorganic complexes,[100] flavins,[101] organic acceptors,[102] and porphyrins.[103] In all these cases, the driving-force dependence of the observed ET rate constant approaches the activationless, diffusion-controlled region, but the decrease in ET rate at high driving force is not clearly observed. For example, McLendon (GM) et al. have investigated the ET quenching of the $^3\pi\pi^*$ excited state of $^*Zn^{II}$-substituted cyt c with a homologous series of viologen dications of varying reduction potentials.[102] The ET rates show a monotonic increase up to driving forces of $\sim$0.7 eV. Figure 6 shows the driving-force dependence of the rate constants (solid curve) calculated from eqs 3–10, along with GM's experimental data. The calculation was performed with exactly the same parameters utilized above for the Ru^{II} diimine complexes, except that the appropriate driving force for the reaction was used and the average radius of the organic acceptors was 3.5 Å as compared to the 6.5 Å radius of the Ru^{II} complexes. The observed rate data for the viologen system are fitted extremely well by the calculated curve. Because the same value for the electronic coupling was used for Figures 5 and 6, this result suggests that the organic viologen and inorganic Ru^{II} diimine acceptors react at the same location on the protein surface and at approximately the same edge-to-edge ET distances. This congruence in the ET pathways is not surprising in view of the similarity of the electrostatic charges, aromaticity, and hydrophobicity of the two classes of acceptors. Inspection of Figures 5 and 6 reveals that the driving forces needed to attain the inverted region for the Zn^{II}cyt c/viologen reaction is $\sim$0.2 eV greater than that for the $^*Ru^{II}$ diimines with cyt c. This shift of the parabolic free energy curve to greater free

(100) English, A. M.; Lum, V. R.; Delaive, P. J.; Gray, H. B. *J. Am. Chem. Soc.* **1982**, *104*, 870.

(101) (a) Meyer, T. E.; Watkins, J. A.; Przysiecki, C. T.; Tollin, G.; Cusanovich, M. A. *Biochemistry* **1984**, *23*, 4761. (b) Tollin, G.; Cheddar, G.; Watkins, J. A.; Meyer, T. E.; Cusanovich, M. A. *Biochemistry* **1984**, *23*, 6345.

(102) Magner, E.; McLendon, G. *J. Phys. Chem.* **1989**, *93*, 7130.

(103) (a) Cho, K. C.; Che, C. M.; Ng, K. M.; Choy, C. L. *J. Am. Chem. Soc.* **1986**, *108*, 2814. (b) Cho, K. C.; Ng, K. M.; Choy, C. L.; Che, C. M. *Chem. Phys. Lett.* **1986**, *129*, 521.

Figure 7. Semilog plot of the calculated k_{obs} (solid curve) for the reaction of $^*Ru(diMeO\text{-}phen)_3^{2+}$ and Fe^{II}cyt c ($\Delta G = -0.69$ V). Equations 3–10 were evaluated from $r = \infty$ to the distance specified on the x-axis. The opposing contributions of k_{act} (dashed curve) and k_{diff} (dotted line) to k_{obs} result in a maximum ET rate constant that occurs at a distance between the donor and acceptor larger than contact.

energies stems from the smaller radii of the viologen reactants, which consequently engenders a larger solvent reorganization energy. On this basis, we expect that the bimolecular rate constant for the reaction of $^*Zn^{II}$cyt c with viologens will diminish for acceptors possessing reduction potentials more positive than +0.3 V vs SCE ($-\Delta G° = 1.2$ V). Analysis of the bimolecular ET kinetics for the reaction of cyt c with flavins leads to similar conclusions[101] and also accounts for the inability to observe inverted-region ET effects in these systems.

The analysis presented here underscores the necessity to consider bimolecular ET occurring over a range of distances. Although the bimolecular reaction is conducted in a solvent with a high dielectric constant and at a relatively high ionic strength, the large positive charge of cyt c gives rise to an appreciable intermolecular potential (eq 4) that can inhibit the ET reaction at distances of close approach. This is illustrated for the reaction of $^*Ru(diMeO\text{-}phen)_3^{2+}$ with Fe^{II}cyt c. Figure 7 graphically depicts the calculated rate constants k_{act}, k_{diff}, and k_{obs} for this bimolecular reaction by integrating eqs 3 and 6 to a distance of r. For the like-charged reactants, there is an increase in k_{diff} with increasing r that is opposed by a decrease in k_{act} owing to poorer electronic coupling (eq 10) of the ET event. From eq 2, these opposing effects lead to a rate maximum at distances greater than contact. This disparate behavior in k_{diff} and k_{act} and their relative contributions to the fastest observed rates of bimolecular ET emphasize the importance of choosing a homologous series of ET partners. Moreover, because the approach of oppositely charged reactants is governed by a favorable electrostatic potential and would result in an increasing rate of reaction to a distance of reactant contact, this analysis suggests that care must be taken when comparing bimolecular ET reactions of cyt c with reactants of dissimilar charge.[103]

In conclusion, the ET rate constants for the photoinduced bimolecular reaction between $^*Ru^{II}$ diimine complexes and cyt c decrease at high driving forces. Our ability to observe the inverted region arises from displacing the Marcus curve vertically below the diffusion limit and shifting it horizontally to lower driving forces. The intramolecular reorganization energies for both reactants are minimal, and the modest reorganization energies associated with solvent lead to a shift of the maximum of the Marcus curve to lower driving forces. This displacement

is coupled with a shift of the Marcus curve to intrinsically slower ET rates resulting from the weak electronic coupling for ET pathways at distances greater than close contact (see Figure 7). In the case here, the inverted-region effect is modest because the intervening excited state of the protein prevents driving forces greater than -1.3 V from being attained. Notwithstanding the approach described here to unveil the inverted region for bimolecular ET reactions is not unique to cyt *c* and such effects may be observed in other systems in which the electronic coupling and reorganization energy are correctly adjusted so that the Marcus curve emerges from the diffusion limit.